American Mineralogist, Volume 76, pages 1872–1883, 1991

Stepwise dehydration of heulandite-clinoptilolite from Succor Creek, Oregon, U.S.A.: A single-crystal X-ray study at 100 K

Thomas Armbruster
Laboratorium für chemische und mineralogische Kristallographie, Universität Bern, Freiestrasse 3, CH-3012 Bern, Switzerland

Mickey E. Gunter
Department of Geology and Geological Engineering, University of Idaho, Moscow, Idaho 83843, U.S.A.

Abstract

The crystal structures of a natural heulandite-clinoptilolite sample and four partially dehydrated phases of the same single crystal have been refined at 100 K in space group $C2/m$ using single-crystal X-ray diffraction data (R = 3.5% for the natural sample and ranges from 3.6 to 5.8% for the dehydrated phases). The chemical formula is $Ca_{2.1}Mg_{0.3}Na_{2.5}K_{0.28}Al_{8.0}Si_{28.2}O_{72}\cdot nH_2O$, where n decreases because of dehydration from 25.5 (ca.) for the natural sample to 17.6, 16.7, and approximately 4–5, respectively, for the dehydrated phases. The unit cell for the natural sample at 100 K has dimensions a = 17.640 Å, b = 17.940 Å, c = 7.405 Å, and β = 116.53°. The cell parameters decreased as dehydration increased with a, b, and c changing by 3.6%, 7.1%, and 0.7%, respectively, whereas β varied unsystematically from 116.52° to 116.44°. Dehydration started with loss of H_2O coordinated to Na in channels defined by ten-membered tetrahedral rings and continued with loss of H_2O not coordinated to cations. As H_2O coordinating Na was expelled, Na migrated to the cavity wall. In a second dehydration step, O-H_2O coordination of Ca in the channels defined by eight-membered tetrahedral rings decreased from eight to seven. In the most dehydrated phase, Ca became six-coordinated. The last dehydration step was accompanied by a strong compression of the channel system, but the tetrahedral topology was preserved.

Introduction

Clinoptilolite and heulandite are monoclinic zeolite minerals characterized by large, intersecting open channels of ten- and eight-membered tetrahedral rings. The large ten-membered A ring (opening 7.05 × 4.25 Å, ca.) and the smaller eight-membered B ring (opening 4.6 × 3.96 Å, ca.) confine channels parallel to **c**. Type-C channels running parallel to **a** are also formed by eight-membered rings and connect A and B channels (Merkle and Slaughter, 1968). The channels are occupied by Na, K, Ca, and H_2O. Charge balance is achieved by variable Al → Si substitution in the tetrahedral framework. Chemical data have been used to distinguish clinoptilolite, $(Na,K)_6(Al_6Si_{30}O_{72})\cdot 20H_2O$ from heulandite, $(Na,K)Ca_4(Al_9Si_{27}O_{72})\cdot 24H_2O$. One definition of clinoptilolite requires that Si/Al > 4.0 (Boles, 1972); another requires that (Na + K) > Ca (Mason and Sand, 1960).

Clinoptilolite is one of the most abundant and economically important natural zeolites mainly because of its cation-exchange properties (Mumpton, 1988). It has been used for the removal of radioactive Cs and Sr from low-level waste streams of nuclear installations and ammonium extraction from sewage and agricultural effluents (review of literature in Mumpton, 1978). Other applications are as dietary supplements in animal husbandry, for absorptive removal of S organic compounds in oil (Benashvili et al., 1988), and O enrichment of air (Galabova and Haralampiev, 1988).

Structures of untreated clinoptilolite have been determined to date on samples from only four localities: Agoura, California, and Alpe di Siusi, Italy (Alberti, 1975); Agoura, California, and Kuruma Pass, Japan (Koyama and Takéuchi, 1977); and recently Richardson Ranch, Oregon (Smyth et al., 1990). The latter sample was also structurally studied in its Cs-exchanged form. The structures of untreated heulandite samples were investigated by Merkle and Slaughter (1968), Alberti (1972), Bresciani-Pahor et al. (1980), Alberti and Vezzalini (1983), and Hambley and Taylor (1984). The structures of K-exchanged heulandite and its high-temperature dehydration product were reported by Galli et al. (1983), and the structure of partially NH_4-exchanged heulandite was investigated by Mortier and Pearce (1981); however, the exact NH_4 position could not be resolved. Bresciani-Pahor et al. (1980) also studied partially Ag-exchanged heulandite. There has been a long-standing discussion of whether clinoptilolite and heulandite crystallize in a truly centric lattice or the symmetry is only pseudocentric (Merkle and Slaughter,

0003–004X/91/1112–1872$02.00

TABLE 1. Data measurement and refinement parameters for heulandite-clinoptilolite from Succor Creek at 100 K

Composition	$Ca_{2.1}Mg_{0.3}Na_{2.5}K_{0.28}Al_{8.0}Si_{28.2}O_{72}\cdot 21.9H_2O$				
Crystal size	0.16 × 0.32 × 0.41 mm				
Space group	*C2/m*				
Radiation	Mo$K\alpha$				
Scan type	ω				
Sample name*	natural	dehyd1	dehyd2	dehyd3	dehyd4
Scan width	1.5°	1.5°	1.5°	1.5°	8.0°
a (Å)	17.640(2)	17.628(2)	17.607(2)	17.576(4)	17.00(1)
b (Å)	17.940(2)	17.902(4)	17.692(4)	17.580(1)	16.66(1)
c (Å)	7.405(3)	7.403(2)	7.412(3)	7.403(3)	7.350(5)
β (°)	116.53(3)	116.52(2)	116.84(3)	116.97(3)	116.44(6)
Maximum θ (°)	26	32	35	25	25
Measured reflections	2072	3378	5442	1919	1775
Unique reflections	1902	3281	4465	1857	1617
Observed reflections >3σ	1752	2945	3672	1709	1338
No. of parameters	212	215	199	194	149
R (%)	3.56	3.65	3.92	4.19	5.8
R_w (%)	3.85	4.00	4.11	4.25	6.2

Note: $R = \Sigma||F_{obs}| - |F_{calc}||/\Sigma|F_{obs}|$, $R_w = (\Sigma w(|F_{obs}| - |F_{calc}|)^2/\Sigma w|F_{obs}|^2)^{1/2}$.
* Dehyd5: $a = 17.63(1)$, $b = 17.91(1)$, $c = 7.406(3)$ Å, $\beta = 116.44(5)°$, cell parameters only.

1968; Alberti, 1972). Merkle and Slaughter (1968) refined heulandite in the acentric space group *Cm*, whereas most other authors preferred the centric space group *C2/m*, mainly to avoid correlation problems in the least-squares refinement.

Bish (1984, 1988) studied the effects of exchanged cations in thermal expansion-contraction and dehydration of clinoptilolite above room temperature. He found cell parameters, and thus the crystal structure, sensitive to exchangeable cations. He also noted the unit-cell dimensions are sensitive to changes in both temperature and relative humidity. The dehydration behavior also strongly depends on the chemical species of the exchanged cations (Bish, 1988).

There have been no low-temperature structure refinements on clinoptilolite or heulandite. Thus our initial aim was to perform a structure study at 100 K on heulandite-clinoptilolite to obtain a better resolution of channel occupants resulting from their reduced thermal motion. However, we quickly found Bish's observation on humidity sensitivity to be true. Our original sample became partly dehydrated when placed in a stream of dry N_2 at 298 K on the X-ray diffractometer prior to data measurement. At this point, the course of our experiment changed. We still performed the refinement at 100 K on a completely hydrated sample, but we also conducted a set of stepwise dehydration experiments and refined four structures having different hydration states.

EXPERIMENTAL PROCEDURE

The heulandite-clinoptilote sample is from Succor Creek, Malheur County, Oregon, provided by the U.S. National Museum (no. 160671). The composition, $Ca_{2.1}Mg_{0.3}Na_{2.5}K_{0.28}Al_8Si_{28.2}O_{72}\cdot 20.9H_2O$, was determined by an ARL-EMX-SM electron microprobe operating at 15 kV and 20 nA. The electron beam was defocused to approximately 20 μm. The approximate H_2O content was estimated by difference and is probably too low, as the sample was analyzed under a vacuum. A second harmonic generation powder test indicated the sample was centric, thus justifying refinement in space group *C2/m*.

Single-crystal experiment

Single-crystal X-ray data were obtained at 100 K with an Enraf-Nonius CAD-4 diffractometer (graphite-monochromatized Mo$K\alpha$ radiation) using a conventional liquid-N_2 cooling device. Additional experimental details for the data measurements and the structure refinements are given in Table 1.

Structure refinements were performed on a fully hydrated sample (labeled "natural") and four partially dehydrated phases of the same single crystal. Differing dehydration states (dehyd1, dehyd2, dehyd3, dehyd4) were obtained by placing the crystal in different gaseous atmospheres at different temperatures for different lengths of time (Table 2). There was a continuous progression of the dehydration process. For instance, dehyd4 was created by placing dehyd3 at 448 K in a dry N_2 stream for 1 h.

With the exception of dehyd4 and dehyd5, cell dimensions were refined from reflections with $32° > \theta > 25°$. For dehyd4 and dehyd5, reflections with $15° > \theta > 10°$ were used. In the experiments natural-dehyd3, the crystal remained transparent and did not change its X-ray scattering characteristics. Dehyd4 turned milky white and developed a strong mosaic pattern. The X-ray reflections became strongly streaked along the ω direction; thus an

TABLE 2. Dehydration conditions for heulandite-clinoptilolite

Sample	*T* (K)	Relative humidity	Time
dehyd1	293	10–20%	10 d
dehyd2	293	0 (N_2)*	12 h
dehyd3	373	0 (N_2)*	6 h
dehyd4	448	0 (N_2)*	1 h
dehyd5	473	dry air	4 h
and**	293	60%	1 min

* Assumed humidity based upon H_2O content of bottled N_2 gas.
** Dehyd5 underwent two dehydration conditions.

8° ω scan was necessary to obtain whole diffraction intensities. The streaked reflections are also responsible for the low precision of the cell dimensions for dehyd4 and dehyd5.

Absorption was tested by ψ scans, but the effect was considered insignificant and the correction was not applied. Data reduction, including background and Lorentz-polarization corrections, was carried out using the SDP (Enraf-Nonius, 1983) program library. Starting parameters were obtained from the program SHELXS-86 (Sheldrick, 1986). The program SHELX76 (Sheldrick, 1976) was applied for structure refinement using unit weights. Neutral-atom scattering factors and real as well as imaginary anomalous dispersion corrections were used.

In test refinement cycles, Si scattering factors were applied for tetrahedral cations. Resulting T-O distances were used to estimate the Si/(Al + Si) ratio for each site using the same method as Koyama and Takéuchi (1977). Corresponding Si, Al scattering factors were introduced for the tetrahedral cations in the subsequent refinement cycles. For framework atoms we followed the nomenclature of Koyama and Takéuchi (1977). Channel positions were labeled by an identifier composed of the applied scattering factor and a number also used by the above authors. Additional numbers were used for new channel positions. For H_2O positions the characteristic number was increased by ten: O1 to O10 are framework positions, O11 to O20 are channel sites (Hambley and Taylor, 1984).

Results

Judging from the Si/Al ratio our sample is heulandite, but the chemical composition of the channel cations suggests it should be considered clinoptilolite. According to the mole plot of Alietti et al. (1977), the chemical composition classifies this sample as heulandite-clinoptilolite for which a thermal behavior of "type 2" should be expected. X-ray powder diffraction experiments similar to Mumpton's (1960), which is the most widely accepted method to differentiate heulandite and clinoptilolite, indicated our sample to be clinoptilolite. Thus we concluded our sample is intermediate heulandite-clinoptilolite.

Partial dehydration of heulandite-clinoptilolite

Dehydration of heulandite-clinoptilolite can be monitored with the cell parameters. With loss of H_2O (natural-dehyd3), b decreased strongly, a decreased slightly, c remained more or less invariant, and β increased slightly. For dehyd4, a and b decreased rapidly (Table 1) which is characteristic of the B phase or heat-collapsed structure of heulandite (Alberti, 1973). For the heat-collapsed phase, β decreased slightly. Rough estimations based on site-occupancy refinement of H_2O indicated the natural sample stored in high humidity had about 25.5 H_2O molecules per formula unit (pfu), differing from the 21.9 molecules as determined by difference from electron microprobe data (Table 1). Flushing the crystal with dry N_2 at room temperature reduced H_2O to 17.6 molecules pfu (dehyd2); prolonged heating at 373 K under N_2 reduced H_2O to 16.7 molecules pfu (dehyd3); and after only 1 h at 448 K, H_2O decreased to 4–5 molecules pfu (dehyd4). In the heat-collapsed phase (dehyd4), the crystal developed numerous cracks. When exposed briefly to humid air at room temperature (humidity 60%), the crystal rehydrated, as determined by the cell dimensions. Dehyd5 cell parameters returned to the original values of the untreated crystal, whereas the mosaic fracture pattern of the crystal persisted.

During all experiments the T-O-T linkage remained unaffected, although various T-O-T angles changed dramatically, especially when going from dehyd3 to dehyd4 (Fig. 1). In the following section we distinguish between dehydration of the natural sample and the heat-collapsed phase found for dehyd4. Observed and calculated structure factors for all structures are given in Table 3[1], positional parameters are summarized in Table 4, and anisotropic displacement parameters are listed in Table 5. Table 6 contains T-O distances, estimated Al concentrations on T sites, T-O-T angles, and M-O distances for channel cations.

Natural sample. In agreement with Koyama and Takéuchi (1977), four metal sites (Na1, Ca2, K3, Mg4) were resolved in the fully hydrated sample (natural) within the channel system. Difference-Fourier maps indicated an additional peak 0.5 Å along **c** from Ca2. This new site was labeled Ca21. We are, however, not sure whether it is a metal position or H_2O. The observed population on Ca2 and Ca21 (Table 4) is below the analytically determined Ca concentration. On the other hand, the population on Na1 is significantly high if compared with the analyses from the electron microprobe; thus some Ca must be assigned to Na1. As a rule, Ca has a scattering power for X-rays twice that of Na. Thus two Na atoms may be counted as one Ca in site-occupancy refinements. The following model is in good agreement with the electron microprobe analyses. If we assume only Ca2 (and not Ca21) represents a Ca site, then 1.5 Ca (pfu) would satisfy the observed population of 0.37. The Na1 site contains all Na + Mg (2.8 pfu), which would explain a population of 0.70 on this site (observed value 1.02). Using the above rule for Ca → Na substitution, the excess of 0.32 in the observed population was explained by 0.16 Ca on site Na1. Thus Ca on Ca2 and Na1 adds to 2.1 pfu exactly the value determined by electron microprobe analysis.

Most Na1 (occupancy, 0.70 Na + Mg, 0.16 Ca) is seven-coordinated by two O neighbors of the tetrahedral framework (O2) and five H_2O molecules (O11, O12, O16, 2 × O15) (Fig. 2). A similar coordination may also be achieved by partial occupancy of O16′ (general position) instead of O16 (on the mirror plane).

The maximum occupancy of Ca2 is 50% because of a clash with an adjacent $(-x,-y,-z)$ unit. For all refinements the determined Ca population converged to values

[1] A copy of Tables 3 and 5 may be ordered as Document AM-91-474 from the Business Office, Mineralogical Society of America, 1130 Seventeenth Street NW, Suite 330, Washington, DC 20036, U.S.A. Please remit $5.00 in advance for the microfiche.

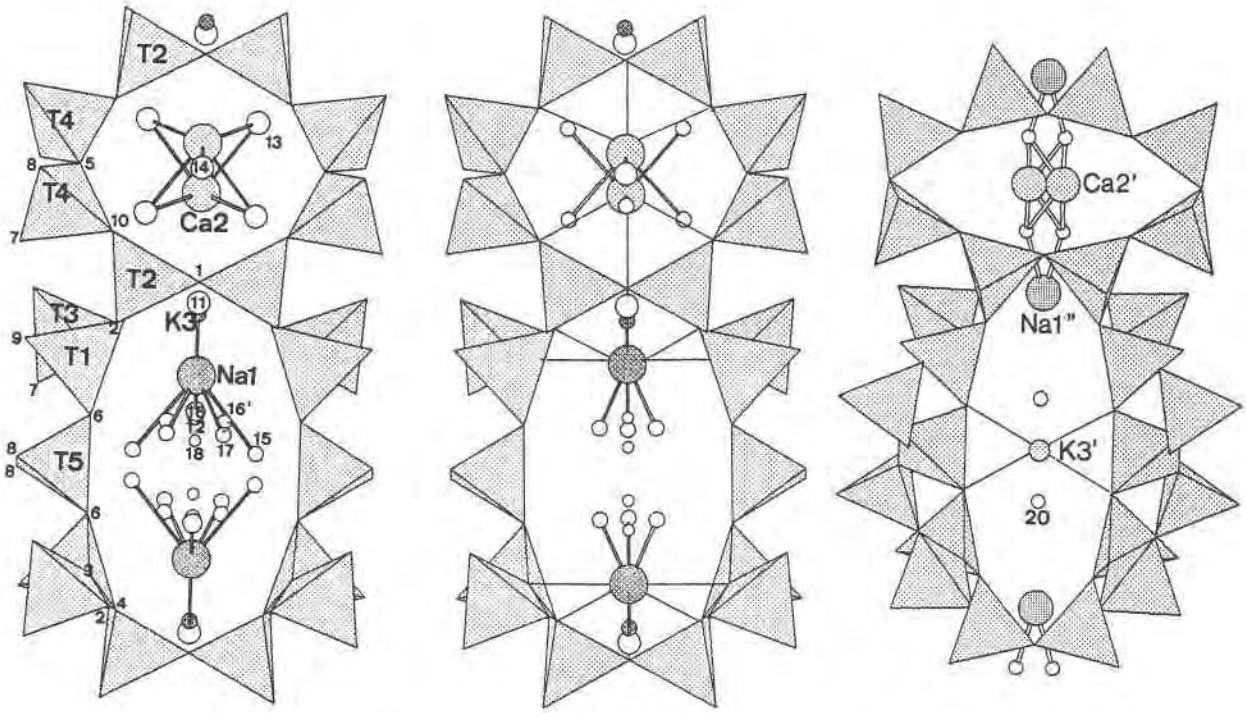

Fig. 1. Projection along [001], displaying the larger A channel confined by ten tetrahedra and the B channel confined by eight-membered rings. (**Left**) sample natural; (**middle**) sample dehyd2; (**right**) dehyd4 (heat-collapsed phase).

significantly below this upper limit. We focus discussion on the Ca2 site that is more highly populated and ignore Ca21 because of the questionable Ca assignment. In the natural sample, Ca2 is eight-coordinated (Fig. 2) with three O atoms (2 × O10, and O1) from the tetrahedral framework and five H_2O molcules (4 × O13 and 1 × O14).

All K was attributed to the K3 site in the center of an eight-membered ring of tetrahedra (type-C channel). K3 is bonded to six framework O atoms (2 × O2, 2 × O3, 2 × O4). The nine- or tenfold coordination is completed by H_2O molecules with O atoms O12 (or 2 × O17) and 2 × O13. Close to K3 (occupancy 7%) is also a H_2O site (O11) that can only be 93% occupied because of a clash with K3. In test refinements O11 converged at 100% occupancy; thus it was fixed at this concentration.

The Mg4 site, not bonded to framework O atoms, was modeled with Mg scattering factors. The low population for this position does not allow a proper coordination to be defined.

O18, with an occupancy of about 10%, is not coordinated to Na1, Ca2, or K3 but survived heating to 393 K under N_2 (dehyd3). Thus this position may actually represent a metal site.

Dehyd1, dehyd2, and dehyd3. Site-occupancy refinements indicated H_2O on O15 (coordinated to Na1) was expelled first, reducing its population from 40% (natural) to 33% (dehyd1) to 6% (dehyd2). In a second step, H_2O on O16 (coordinated to Na) decreased rapidly from a population of 70% (natural, dehyd1) to 24% (dehyd2). Correlated with the loss of O15 is the observation of two well-resolved metal sites (Na1 and Na1′, 0.52 Å apart) close to M1 of Koyama and Takéuchi (1977). For dehyd1, Na1 showed a higher occupancy than Na1′, and in dehyd2, with only 6% occupancy on O15, this ratio became reversed. Na1′ is assumed to be eightfold coordinated (Fig. 2). When partly dehydrated, most Na migrated to this site, and the loss of H_2O (O15, O17, O12) was compensated by the five framework O sites (O1, 2 × O2, 2 × O3) close to Na1′. In other words, Na1′ nestled close to the cavity wall, balancing the loss of coordinating H_2O. In the first dehydration step from natural to dehyd1, only the Na1 coordination was influenced, and Ca2 did not become involved until dehydration from dehyd1 to dehyd2.

In the partially dehydrated crystal (dehyd2), the amount of H_2O on O13 decreased, and it moved to two different sites: O13 (general position) and O13′ (on a mirror plane). The population of O12 decreased from 60% (ca.) (natural, dehyd1) to 40% (dehyd2). All other H_2O positions changed no more than 10% or remained uninfluenced. In dehyd2, only Ca2 survived, whereas Ca21 disappeared. Owing to the loss of some H_2O on O13 and rearrangement to the new site O13′, the coordination of Ca decreased from eight to seven (2 × O10, 2 × O13, O1, O14, O13′) (Fig. 2) and the populations of Na1 and Na1′ were significantly lower than in dehyd1 or natural; thus some cations were probably dispersed in the channel.

The major characteristics of dehyd3 are as follows: O17 became vacant, O15 had only a very low occupancy of approximately 3%, and the Na1-type site split into Na1′

TABLE 4. Occupancies, positional parameters, and B_{eq} values of heulandite-clinoptilolite from Succor Creek at 100 K

Sample	Atom	Occupancy	x	y	z	B_{eq}
Natural	T1	1.0	0.1796(1)	0.1703(1)	0.0941(1)	0.80(2)
dehyd1		1.0	0.17953(4)	0.17019(4)	0.0971(1)	0.737(8)
dehyd2		1.0	0.17980(3)	0.16754(3)	0.0937(1)	0.986(7)
dehyd3		1.0	0.1805(1)	0.1657(1)	0.0945(1)	1.20(2)
dehyd4		1.0	0.1834(1)	0.1513(1)	0.0852(3)	1.63(3)
Natural	T2	1.0	0.2884(1)	0.0899(1)	0.5006(1)	0.83(1)
dehyd1		1.0	0.28884(4)	0.08997(4)	0.5011(1)	0.77(1)
dehyd2		1.0	0.29307(3)	0.09038(3)	0.5050(1)	1.021(7)
dehyd3		1.0	0.2960(1)	0.0903(1)	0.5090(2)	1.28(2)
dehyd4		1.0	0.3251(1)	0.0914(1)	0.5100(3)	1.53(3)
Natural	T3	1.0	0.2926(1)	0.3096(1)	0.2848(1)	0.81(1)
dehyd1		1.0	0.29244(4)	0.30966(4)	0.2845(1)	0.743(9)
dehyd2		1.0	0.28906(3)	0.31107(3)	0.2783(1)	0.989(7)
dehyd3		1.0	0.2873(1)	0.3121(1)	0.2750(2)	1.25(2)
dehyd4		1.0	0.2571(1)	0.3239(1)	0.2433(3)	1.73(3)
Natural	T4	1.0	0.0642(1)	0.2990(1)	0.4097(1)	0.86(1)
dehyd1		1.0	0.06395(4)	0.29883(4)	0.4090(1)	0.788(1)
dehyd2		1.0	0.06393(3)	0.29480(3)	0.4088(1)	1.020(7)
dehyd3		1.0	0.0638(1)	0.2917(1)	0.4088(1)	1.30(2)
dehyd4		1.0	0.0722(1)	0.2567(1)	0.4332(3)	1.51(3)
Natural	T5	1.0	0	0.2139(1)	0	0.89(2)
dehyd1		1.0	0	0.2133(1)	0	0.81(1)
dehyd2		1.0	0	0.20784(4)	0	0.99(1)
dehyd3		1.0	0	0.2045(1)	0	1.20(2)
dehyd4		1.0	0	0.1864(2)	0	1.58(5)
Natural	O1	1.0	0.3039(2)	0	0.5437(6)	2.06(7)
dehyd1		1.0	0.3047(2)	0	0.5443(4)	1.96(4)
dehyd2		1.0	0.3106(2)	0	0.5496(4)	2.93(5)
dehyd3		1.0	0.3160(3)	0	0.5558(7)	3.7(1)
dehyd4		1.0	0.3678(3)	0	0.539(1)	2.3(1)
Natural	O2	1.0	0.2307(2)	0.1198(2)	0.6116(4)	1.93(5)
dehyd1		1.0	0.2307(1)	0.1197(1)	0.6117(3)	1.84(3)
dehyd2		1.0	0.2366(1)	0.1182(1)	0.6206(3)	2.83(3)
dehyd3		1.0	0.2406(2)	0.1167(2)	0.6279(5)	3.66(7)
dehyd4		1.0	0.2992(3)	0.1110(3)	0.6971(7)	2.6(1)
Natural	O3	1.0	0.1818(2)	0.1550(2)	−0.1170(4)	2.01(5)
dehyd1		1.0	0.1811(1)	0.1546(1)	−0.1179(3)	1.91(3)
dehyd2		1.0	0.1828(1)	0.1489(1)	−0.1186(3)	2.30(3)
dehyd3		1.0	0.1853(2)	0.1459(2)	−0.1156(4)	2.53(5)
dehyd4		1.0	0.2110(3)	0.1269(3)	−0.0940(7)	2.7(1)
Natural	O4	1.0	0.2390(2)	0.1073(1)	0.2541(4)	1.77(4)
dehyd1		1.0	0.2400(1)	0.1077(1)	0.2545(3)	1.71(3)
dehyd2		1.0	0.2434(1)	0.1078(1)	0.2592(2)	1.93(2)
dehyd3		1.0	0.2448(2)	0.1072(2)	0.2630(4)	2.26(5)
dehyd4		1.0	0.2403(3)	0.0989(3)	0.2845(7)	2.6(1)
Natural	O5	1.0	0	0.3268(2)	½	2.10(7)
dehyd1		1.0	0	0.3267(2)	½	2.04(5)
dehyd2		1.0	0	0.3208(2)	½	3.14(5)
dehyd3		1.0	0	0.3166(3)	½	4.5(1)
dehyd4		1.0	0	0.2279(5)	½	4.6(2)
Natural	O6	1.0	0.0823(1)	0.1599(1)	0.0666(4)	1.44(4)
dehyd1		1.0	0.0825(1)	0.1593(1)	0.0677(3)	1.38(3)
dehyd2		1.0	0.0829(1)	0.1536(1)	0.0641(2)	1.61(2)
dehyd3		1.0	0.0834(2)	0.1506(2)	0.0626(4)	1.84(5)
dehyd4		1.0	0.0790(3)	0.1287(3)	0.0128(7)	2.2(1)
Natural	O7	1.0	0.3735(2)	0.2655(2)	0.4534(4)	2.49(5)
dehyd1		1.0	0.3729(1)	0.2651(1)	0.4532(3)	2.41(3)
dehyd2		1.0	0.3678(1)	0.2660(1)	0.4506(3)	3.21(3)
dehyd3		1.0	0.3667(2)	0.2684(2)	0.4494(5)	3.93(6)
dehyd4		1.0	0.3389(3)	0.2941(4)	0.4522(8)	3.2(1)
Natural	O8	1.0	0.0072(2)	0.2672(2)	0.1833(4)	1.95(5)
dehyd1		1.0	0.0068(1)	0.2667(1)	0.1831(3)	1.85(3)
dehyd2		1.0	0.0081(1)	0.2613(1)	0.1844(3)	2.35(3)
dehyd3		1.0	0.0087(2)	0.2580(2)	0.1849(4)	2.91(5)
dehyd4		1.0	0.0337(4)	0.2451(4)	0.1915(8)	3.5(1)
Natural	O9	1.0	0.2110(1)	0.2542(1)	0.1787(4)	1.65(4)
dehyd1		1.0	0.2105(1)	0.2547(1)	0.1764(3)	1.50(3)
dehyd2		1.0	0.2079(1)	0.2548(1)	0.1620(2)	1.58(2)
dehyd3		1.0	0.2073(2)	0.2538(2)	0.1580(4)	1.81(4)
dehyd4		1.0	0.1966(3)	0.2472(3)	0.1233(7)	2.4(1)
Natural	O10	1.0	0.1155(2)	0.3723(1)	0.3963(4)	1.84(4)
dehyd1		1.0	0.1147(1)	0.3724(1)	0.3938(3)	1.72(3)
dehyd2		1.0	0.1101(1)	0.3721(1)	0.3899(3)	2.23(3)
dehyd3		1.0	0.1081(2)	0.3701(2)	0.3880(4)	2.83(5)
dehyd4		1.0	0.0925(3)	0.3517(3)	0.4787(8)	2.71(1)

TABLE 4—*Continued*

Sample	Atom	Occupancy	x	y	z	B_{eq}
Natural	Na1	1.02(1)	0.1543(2)	0	0.6688(4)	4.45(8)
dehyd1		0.74(4)	0.1496(9)	0	0.6672(5)	2.9(1)
dehyd2		0.12(1)	0.138(2)	0	0.670(4)	3.95*
dehyd3			vacant			
dehyd4			vacant			
Natural	Na1′		vacant			
dehyd1		0.32(1)	0.181(1)	0	0.682(2)	2.37*
dehyd2		0.70(1)	0.1838(4)	0	0.7263(8)	5.2(1)
dehyd3		0.66(1)	0.1914(3)	0	0.7517(8)	3.8(1)
dehyd4			vacant			
dehyd3	Na1″	0.12(1)	0.254(2)	0	0.843(6)	3.95*
dehyd4		0.60(2)	0.2977(7)	0	0.940(2)	4.0(3)
Natural	Ca2	0.37(2)	0.4592(2)	0	0.804(1)	1.8(1)
dehyd1		0.33(1)	0.4596(2)	0	0.8057(9)	1.46(5)
dehyd2		0.386(2)	0.4663(1)	0	0.7626(3)	2.60(3)
dehyd3		0.33(1)	0.4697(3)	0	0.7577(7)	3.2(1)
dehyd4	Ca2′	0.44(1)	½	−0.0295	½	5.8(2)
Natural	Ca21	0.10(2)	0.466(2)	0	0.739(7)	4.2(7)
dehyd1		0.12(1)	0.4646(6)	0	0.743(3)	2.5(2)
Natural	K3	0.07	0.743(1)	0	0.072(3)	1.6(4)
dehyd1		0.07	0.7430(9)	0	0.075(2)	1.8(2)
dehyd2		0.05	0.743(1)	0	0.057(2)	1.1(2)*
dehyd3		0.18	0.7447(8)	0	0.059(2)	3.29*
dehyd4	K3′	0.26(2)	0	0	0	4.0(3)
Natural	Mg4	0.04(1)	0	0	½	3.95*
dehyd1		0.08(1)	0	0	½	3.95*
dehyd2		0.05(1)	0	0	½	3.95*
dehyd3			vacant			
Natural	O11	1.0	0.2237(5)	½	−0.001(1)	3.7(1)
dehyd1		1.0	0.2239(3)	½	−0.0027(8)	3.29(9)*
dehyd2		1.0	0.2185(5)	½	−0.006(1)	6.4(2)
dehyd3		0.72(5)	0.204(2)	½	−0.033(5)	8.5(8)
Natural	O12	0.60(3)	0.0841(9)	0	0.875(4)	11.9(7)
dehyd1		0.56(2)	0.0833(9)	0	0.871(4)	13.4(7)
dehyd2		0.40(1)	0.0741(6)	0	0.873(2)	5.8(3)
dehyd3		0.47(2)	0.0789(8)	0	0.868(2)	5.8(3)
Natural	O13	1.0	0.0778(2)	0.4196(2)	0.9672(6)	4.89(8)
dehyd1		1.0	0.0779(2)	0.4193(2)	0.9672(5)	4.67(6)
dehyd2		0.58(1)	0.0757(4)	0.4150(4)	0.9591(9)	8.1(1)
dehyd3		0.62(2)	0.080(1)	0.4147(8)	0.953(2)	20.2(5)
dehyd2	O13′	0.43(2)	0.053(2)	½	0.952(4)	18.3(15)*
dehyd3		0.38(4)	0.028(4)	½	0.930(9)	19.7(1)*
Natural	O14	1.0	0	½	½	5.9(2)
dehyd1		1.0	0	½	½	5.7(2)
dehyd2		1.0	0	½	½	7.8(2)
dehyd3		1.0	0	½	½	12.2(5)
Natural	O15	0.40(1)	−0.0262(7)	0.0899(7)	0.508(3)	8.1(4)
dehyd1		0.33(1)	−0.0264(7)	0.0893(6)	0.509(3)	7.3(3)
dehyd2		0.06(1)	−0.024(2)	0.095(2)	0.501(7)	3.95*
dehyd3		0.03(1)	0.05(1)	0.04(1)	0.56(2)	3.95*
Natural	O16	0.69(2)	0.0941(6)	0	0.272(2)	6.0(3)
dehyd1		0.70(2)	0.0940(5)	0	0.276(1)	5.3(2)
dehyd2		0.24(2)	0.092(1)	0	0.307(3)	4.8(4)
dehyd3		0.15(3)	0.097(2)	0	0.337(9)	5.6(13)
Natural	O16′	0.19(2)	0.423(2)	0.458(2)	0.645(5)	7.27(7)
dehyd1		0.18(1)	0.424(2)	0.542(2)	0.643(4)	7.87(7)
dehyd2		0.17(1)	0.422(2)	0.537(2)	0.603(5)	10.8(13)*
dehyd3		0.17(2)	0.418(2)	0.536(4)	0.58(1)	13.8(28)*
Natural	O17	0.15(1)	0.058(2)	0.042(2)	0.705(4)	4.3(6)
dehyd1		0.17(1)	0.0582(9)	0.0393(9)	0.706(3)	3.3(3)
dehyd2		0.07(1)	0.059(2)	0.035(2)	0.669(6)	3.95*
dehyd3			vacant			
Natural	O18	0.11(1)	0.045(3)	0	0.085(7)	3.95*
dehyd1		0.10(1)	0.043(3)	0	0.080(6)	3.95*
dehyd2		0.08(1)	0.106(3)	0	0.114(7)	3.95*
dehyd3		0.12(1)	0.108(3)	0	0.119(7)	3.95*
dehyd4	O19	0.37(3)	0.088(2)	0.468(1)	0.840(4)	7.9*
dehyd4	O20	0.19(2)	0.597(3)	½	0.227(7)	3.95*

Note: $B_{eq} = 8/3\ \pi^2\ \Sigma_i\ [\Sigma_j\ (U_{ij} a_i^* a_j^* a_i \% a_j)]$.

* Starred B_{eq} values without estimated standard deviations in parentheses were fixed; those with standard deviations were refined isotropically.

TABLE 6. T-O distances, T-O-T bridging angles, and M-O distances for channel cations

	Natural	dehyd1	dehyd2	dehyd3	dehyd4
T1-O3	1.627(4)	1.627(3)	1.631(3)	1.633(4)	1.634(10)
-O4	1.624(3)	1.624(2)	1.623(2)	1.618(3)	1.607(8)
-O6	1.638(3)	1.637(2)	1.638(2)	1.635(4)	1.654(5)
-O9	1.622(3)	1.625(2)	1.632(2)	1.625(4)	1.621(5)
Average	1.628	1.628	1.631	1.628	1.629
Al content 21%					
T2-O1	1.641(2)	1.640(1)	1.635(1)	1.629(2)	1.660(3)
-O2	1.6548(4)	1.654(2)	1.659(2)	1.648(5)	1.652(11)
-O4	1.663(3)	1.663(2)	1.655(2)	1.652(3)	1.647(8)
-O10	1.661(3)	1.663(2)	1.660(2)	1.656(5)	1.663(6)
Average	1.656	1.655	1.652	1.646	1.656
Al content 39%					
T3-O2	1.624(4)	1.620(2)	1.624(2)	1.626(4)	1.630(6)
-O3	1.631(4)	1.630(2)	1.636(2)	1.638(4)	1.643(9)
-O7	1.621(3)	1.619(2)	1.610(2)	1.604(3)	1.624(8)
-O9	1.634(2)	1.630(2)	1.633(2)	1.635(4)	1.631(5)
Average	1.628	1.625	1.626	1.626	1.632
Al content 18%					
T4-O5	1.629(2)	1.628(2)	1.619(1)	1.610(2)	1.586(4)
-O7	1.605(3)	1.604(2)	1.600(2)	1.596(3)	1.605(5)
-O8	1.625(3)	1.622(2)	1.615(2)	1.607(3)	1.608(11)
-O10	1.623(3)	1.624(2)	1.630(2)	1.624(4)	1.624(4)
Average	1.621	1.620	1.616	1.609	1.606
Al content 16%					
T5-O6 (2×)	1.627(2)	1.624(2)	1.628(2)	1.627(4)	1.620(6)
-O8 (2×)	1.618(4)	1.618(3)	1.615(2)	1.610(4)	1.596(9)
Average	1.622	1.621	1.622	1.619	1.608
Al content 16%					
T2-O1-T2	158.0(3)	157.7(2)	156.3(2)	154.1(3)	133.2(4)
T2-O2-T3	145.8(3)	145.6(2)	145.7(2)	145.4(3)	139.5(3)
T1-O3-T3	144.5(3)	143.9(2)	139.7(2)	138.5(2)	135.5(4)
T1-O4-T2	140.2(3)	140.3(2)	142.6(2)	143.6(3)	149.4(4)
T4-O5-T4	144.4(2)	144.2(2)	147.0(2)	148.4(4)	144.8(5)
T1-O6-T5	135.4(2)	135.0(2)	133.9(1)	133.9(2)	128.8(3)
T3-O7-T4	163.0(2)	163.9(1)	167.3(1)	166.9(2)	150.2(5)
T4-O8-T5	148.6(2)	148.4(2)	150.1(1)	150.8(2)	149.0(5)
T1-O9-T3	145.4(2)	145.0(1)	144.3(1)	144.8(2)	150.6(3)
T2-O10-T4	141.7(2)	140.8(1)	137.9(1)	138.1(2)	131.6(4)
Na1-O2 (2×)	2.667(4)	2.71(1)	2.84(3)		
-O11	2.437(7)	2.489(9)	2.62(2)		
-O12	2.36(3)	2.27(3)	2.25(4)		
-O15 (2×)	2.60(1)	2.53(1)	2.49(4)		
-O16	2.64(1)	2.61(1)	2.44(3)		
[-O16′ (2×)	2.24(3)	2.19(3)]			
Na1′-O1		2.79(3)	3.056(9)		
-O2 (2×)		2.46(1)	2.552(5)	2.549(6)	
-O3 (2×)		3.135(9)	2.878(3)	2.76(4)	
-O11		2.21(1)	2.010(9)	1.87(2)	
-O12		2.65(4)	2.61(2)	2.49(2)	
[-O17 (2×)		2.65(4)	2.13(4)]		
-O16		2.70(2)	2.78(2)	2.74(5)	
[-O16′ (2×)		2.40(3)	2.40(3)	2.37(5)]	
Na1″-O1				2.80(4)	
-O2 (2×)				2.54(2)	2.58(1)
-O3 (2×)				2.91(2)	2.53(1)
-O13 (2×)				3.01(3)	
-O19 (2×)					1.97(2)
Ca2-O1	2.551(6)	2.543(4)	2.470(3)	2.425(6)	
-O10 (2×)	2.725(4)	2.715(3)	2.615(2)	2.630(4)	
-O13 (2×)	2.381(4)	2.371(4)	2.358(6)	2.35(1)	
-O13a (2×)	2.526(9)	2.516(7)			
-O14	2.65(1)	2.659(7)	2.276(2)	2.199(6)	
-O13′			2.29(4)	2.30(7)	
Ca2′-O1 (2×)					2.438(8)
-O10 (2×)					2.576(8)
-O19 (2×)					2.49(3)
[-O19a (2×)					2.27(2)]
K3-O2 (2×)	3.11(2)	3.09(1)	3.08(1)	3.02(2)	
-O3 (2×)	2.945(8)	2.937(6)	2.882(7)	2.780(9)	
-O4 (2×)	3.12(2)	3.13(1)	3.11(1)	3.11(2)	
-O17 (2×)	3.01(3)	3.00(2)	3.19(4)		
[-O12	2.66(3)	2.66(2)	3.0(1)]	2.91(3)	
-O13 (2×)	3.23(2)	3.23(1)	3.09(2)	3.02(3)	
[-O13′			3.08(4)	3.47(7)]	
K3′-O6 (4×)					2.509(5)
O20-O4 (2×)					2.82(5)
-O6 (2×)					2.60(3)

Note: M-O distances in brackets indicate that they are an alternative possibility to the distances cited directly above.

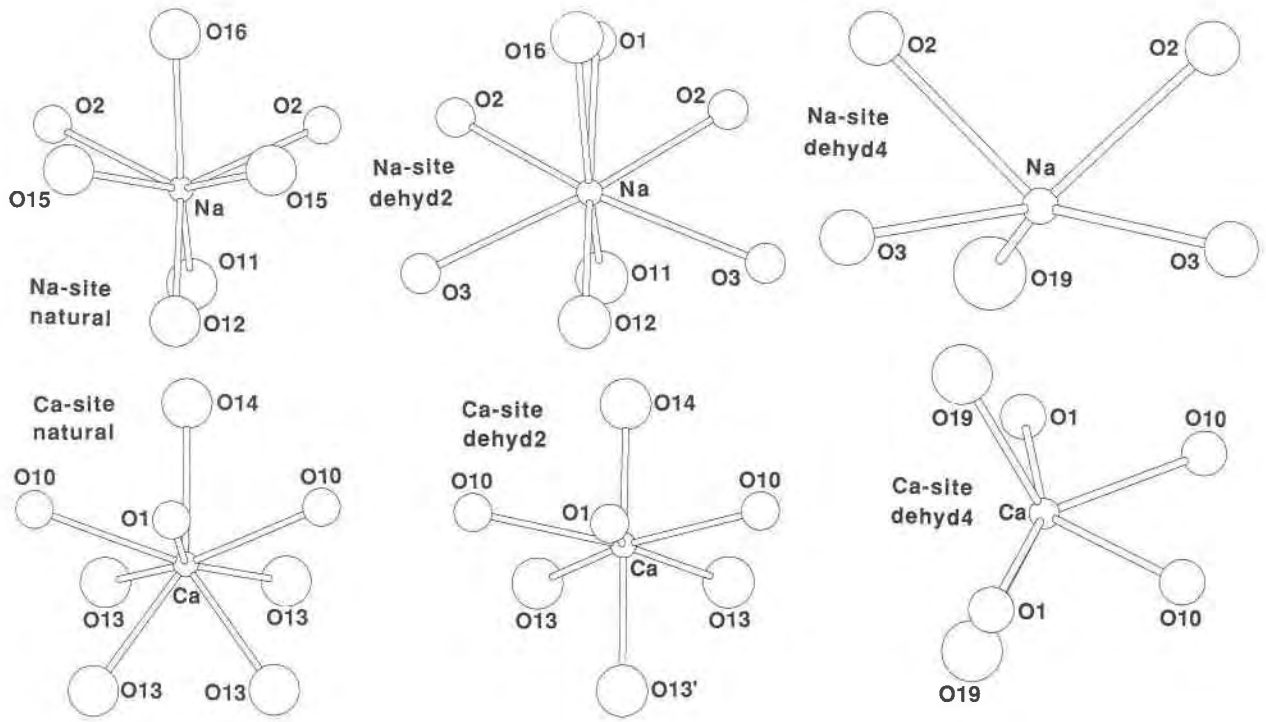

Fig. 2. Variation of channel cation coordination with dehydration projected on (100) and rotated 5° around **c** (natural, dehyd2, dehyd4). **(Upper row)** Na1, **(Lower row)** Ca2.

and Na1″ with the original Na1 position (natural) becoming vacant. This indicates that Na migrated farther along **a** to the channel wall. The population of O11 decreased from 1.0 to 0.72, but simultaneously the population of K3, only 0.5 Å from O11, increased from 7 to 18%. It is not clear whether this is a real effect. For dehyd3 the Na1′-O11 and Na1″-O11 distances became unrealistically short (Table 6). This suggests vacancies and positional disorder of O11, which is also supported by the strong anisotropy of displacement parameters (Table 5). In addition, the number of channel cations on Na1′ and Na1″ decreased significantly below the number for the untreated sample (natural), which could be interpreted by a migration of some cations from Na1 to K3. O13 and O14 were increasingly disordered as indicated by high displacement parameters (Table 5). The coordination of Ca2 remained unaltered, and Mg4 could no longer be located.

Dehyd4. Dehyd4 represents a heat-collapsed structure significantly different from the above four structures. Channel type B changed in cross section from circular (Fig. 1) in natural and dehyd2 to strongly elongated along **b**. This is mainly caused by a migration of O5 along **b** away from the center of channel type B. The angle O5-O10-O5 (Fig. 1) was 143.6° in the natural sample but decreased to 77.3° in dehyd4. This large change, however, had no influence on the T4-O5-T4 bridging angle (Table 6), and only the orientation of the angle changed. With this transition, O1 moved toward the center of channel B and was accompanied by a tilting of T2. The migration of O1 (Fig. 1) is also responsible for the more compressed shape of channel B. The compressed character of the heat-collapsed phase also caused a general decrease of T-O-T angles (Table 6). In the natural sample, these angles vary between 135° and 163°, whereas in the heat-collapsed phase they are between 129° and 151°. The strongest decrease, from 158° to 133°, is observed for T2-O1-T2.

Five well-defined channel positions were found; three are clearly identified as metal sites, one is H_2O, and the species of the fifth is undetermined. Ca migrated to the disordered site Ca2′, which is situated in a B channel on a twofold axis. The disorder reflects the deformation of the channel cross section. Ca2′ is six-coordinated by four framework O atoms (2 × O1, 2 × O10) and two H_2O molecules (2 × O19) (Fig. 2). The population of Ca2′ is significantly greater than the original population in the natural sample (Table 4). Na1 merged with K3 to form the new site Na1″ coordinated to four framework O atoms (2 × O2, 2 × O3). In addition, O19 shows short distances of Na″; thus a sixfold coordination seems possible. Positional disorder of O19 could not be resolved because this site was only refined with a fixed isotropic displacement parameter. K3′, located at the origin, has four framework O atoms (4 × O6) as nearest neighbors.

The new site, O20, is not linked to channel positions but has four framework O atoms (2 × O4, 2 × O6) as nearest O atoms. Thus O20 is probably a cation site because the number of cations found in dehyd4 is less than the number of cations in the natural sample and after

TABLE 7. Channel cations in natural heulandite-clinoptilolite

Name	Σcat total	Σcat 1+	Σcat 2+	K	Reference
Agoura	3.69	1.41	2.28	0.97	Alberti (1975)
Siusi	5.78	4.15	1.64	0.98	Alberti (1975)
Kuruma	4.88	2.81	2.07	0.17	Koyama and Takéuchi (1977)
Agoura	4.89	3.48	1.41	1.68	Koyama and Takéuchi (1977)
Richardson	4.32	2.51	1.81	1.21	Smyth et al. (1990)
Giebelsbach	4.7	0.9	3.9	0.9	Merkle and Slaughter (1968)
Faröer	5.38	1.69	3.69	0.43	Alberti (1972)
Nadap	5.23	1.32	3.91	1.02	Alberti and Vezzalini (1983)
Azerbaijan	4.3	1.2	3.1	0.1	Bresciani-Pahor et al. (1980)
Coonabarabran	3.8	1.5	2.3	—	Hambley and Taylor (1984)
Succor	5.18	2.78	2.4	0.28	this paper

heating to 448 K is is improbable that H_2O molecules are bonded only to framework O atoms by H bonds.

DISCUSSION

Natural sample

Examples of natural (untreated) heulandite-clinoptilolite minerals for which chemical analyses and structure refinements are available are summarized in Table 7. The dominant channel cations are Ca, Na, and K. All structure refinements (see references in Table 7) have two metal positions in common within the channel system: one site in channel A, corresponding to our Na1, and a second site in channel B, corresponding to our Ca2. For compositions with increased K, a third site, corresponding to our K3, becomes important. This third position was first identified by Koyama and Takéuchi (1977) and later confirmed for K-exchanged heulandite (Galli et al. 1983). K3 is only 0.6 Å from the H_2O site O11; thus K3 and O11 are barely resolvable by room-temperature structure refinements. In the most recent refinement of Smyth et al. (1990), the refined population of 64(1)% for K3 is significantly higher than the chemically determined K concentration, which would require a population of 30%. Their K3 also exhibits large displacement parameters, especially along **a** and **c**. On the other hand, Smyth et al. (1990) reported that occupancies of O11 refined to zero. These observations are in agreement with the hypothesis that O on O11 and K on K3 were simulated by one site, their M3. The close association of K3 and O11 is probably also the reason why Alberti (1975) found only O11 but not K3 in his K-rich clinoptilolite samples.

The short distance between K3 and Na1 (1.85 Å) indicates that either Na1 or K3 can be occupied within one cage. The maximum occupancy of Ca2 is 0.5 because of a clash with a neighboring site at $-x,-y,-z$. Thus the maximum concentration of channel cations (Na,K,Ca) in natural heulandite minerals is six atoms pfu. An exception to this upper limit is possible if, instead of Na1, a position close to O18 is occupied by cations. Galli et al. (1983) assigned K to a corresponding site in K-exchanged heulandite. In such a case, up to ten cations can be placed in the channel system. In Table 7, the number of channel cations varies between 3.7 and 5.8. In structures with a large deficit of channel cations, additional H_2O molecules should be expected to fill the empty space. In heulandite from Coonabarabran that is strongly channel-cation depleted (Table 7), Hambley and Taylor (1984) identified a position of O12′ that is not linked to channel cations. Dehydration experiments at 343 K under vacuum preferentially caused this H_2O to be expelled. O12 is only 0.7 Å from O12′ and thus can be easily overlooked when only partially occupied. For our refinement of the sample from Succor Creek that is channel cation rich, anisotropic displacement parameters (Table 5) indicated that O12 is strongly anisotropic with the largest extension along **c**, exactly the direction where O12′ would be expected. After prolonged flushing with dry N_2 (dehyd2), the population and displacement parameters (especially U_{33}) of O12 decreased. This observation confirms that our O12 site (in natural and dehyd1) actually represents a mixture of O12 and O12′ as found by Hambley and Taylor (1984). Resolution of O12′ in our 100 K experiment was not possible because of the low occupancy. If we follow the simple model discussed above that Na1 is occupied by 70% Na and 16% Ca, then O12′ can only be occupied to 14%. A corresponding reduction of the population of O12 was also observed after partial dehydration (dehyd2 and dehyd3).

One should also expect a space-filling H_2O molecule (for vacancies on Ca2) in the type-B channel. It could be assumed that site Ca21 actually represents H_2O. In the natural sample, the population of Ca2 and Ca21 add to 47% (assuming Ca scattering factors). In the dehyd2 sample, Ca2 and Ca21 merged to one site with a population of 39%. This decrease could indicate H_2O loss.

Partial dehydration

Flushing the sample with dry N_2 caused it to become partially dehydrated. Resulting difference-Fourier maps were checked to see if N_2 entered the structure, replacing H_2O; the maps indicated a significant decrease in electron density within the channel system, and no additional electron density resulting from N_2 was observed. Room-temperature N_2 treatment yielded a similar degree of dehydration and H_2O arrangement as obtained by Hambley and Taylor (1984), who used a vacuum (18 h) at 343 K. These experiments all show H_2O content in heulandite-clinoptilolite minerals is strongly dependent on the activity of H_2O.

Hambley and Taylor (1984) observed that after partial dehydration the x and z coordinates of CS1 (our Na1) increased significantly, which can be understood on the basis of our observation, and that with increasing loss of H_2O, cations on the Na1 site moved to the neighboring site Na1′. After partial dehydration, Hambley and Taylor (1984) found a new site, CS3, with an occupancy consistent with the depletion of sites CS1 and CS2. However, no electron density was found at this position in our refinements. In addition, low-temperature data enabled us to locate weakly occupied positions such as K3, O17, O18, and Mg4. In our partially dehydrated crystals, as well as in the one of Hambley and Taylor, the sevenfold coordination of Ca2 (O1, 2 × O10, 2 × O13, O13′, O14) stabilized the almost circular cross section of channel B. A similar result can be derived from the experiments of Galli et al. (1983), who used K-exchanged heulandite (K also occupies a site corresponding to Ca2). When K loses its H_2O coordination, the framework, and especially channel B, is strongly distorted.

The heat-collapsed structure

In the Succor crystal, the compression of the B channel is accompanied by a decrease of the Ca2 coordination from seven (dehyd3) to six (dehyd4). The coordination change is caused by a sudden loss of H_2O on site O14. The resulting heat-collapsed structure is significantly different from the previously refined heat-collapsed heulandite structures. Alberti and Vezzalini (1983) studied a heulandite sample from Nadap before and after 6 h treatment under vacuum at 663 K; they observed that after heating T1-O9-T3 bridges are partially broken. Only the T3 tetrahedron moved to a new site, T3D, with the vertices (O2,O3,O7) and the new fourth vertex (O9D). This O9D vertex (positioned on a mirror plane) is shared by an analogous T3D tetrahedron of an adjacent unit (Fig. 3). Migration of T1 to form a new tetrahedron is prevented by geometrical constraints (Alberti and Vezzalini, 1983). Thus the resulting framework is interrupted, and on the basis of this new knowledge, the previous results of Alberti (1973) were reinterpreted. In his heated Faröer heulandite (heat-collapsed heulandite) the enigmatic X3 site actually represents the T3D position, and 20% of broken T1-O9-T3 bridges were subsequently derived by Alberti and Vezzalini (1983). According to these authors, the driving force for breaking T-O-T bonds is related to the population of cations on CS2 (our Ca2) with high ionic potential. In a dehydrated state cations from CS2 move to a site at 0,½,½ [actually a H_2O site (O14) for natural clinoptilolite and heulandite]. Ca on this new site remains bonded to O1 and attracts O1 strongly toward the center of the B channel. The resulting strain is in turn released by partial breaking of T1-O9-T3 links. Because of new T3D-O9D-T3K links (Fig. 3), the T2-O1-T2 angle is additionally compressed to 118° in the B phase refined by Alberti (1973), whereas 133° was observed for our Succor heat-collapsed phase. In the Succor sample, β first increased (natural-dehyd3) and then decreased 0.5° when the heat-collapsed phase was formed, whereas β of the Nadap heulandite of Alberti and Vezzalini (1983) increased about 2° in the B phase. An additional strong decrease was observed for c, which contracts from 7.430(2) to 7.255(2) Å in the Nadap sample.

This B phase with an altered framework topology (e.g., sample from Nadap) maintains its shorter dimensions and does not rehydrate immediately if brought back to room conditions. Partial rehydration is observed only after months (Gottardi and Galli, 1985). In contrast, our heat-collapsed phase shows the same tetrahedral framework topology as the natural sample and also completely rehydrates within seconds. This behavior agrees with a "heulandite type 2" defined by Alietti (1972). The fact that Alietti (1972) observed the presence of two or more phases after heat treatment of such "type 2" heulandite samples may be explained by the higher temperature at which domains with altered tetrahedral topology (in the sense of Alberti and Vezzalini, 1983) were formed. These structural variants rehydrate only sluggishly, whereas domains that maintain the type-A topology (as in this study) rehydrate much faster. This investigation also shows that this transformation can occur at significantly lower temperatures than hitherto assumed. Under such conditions, the activation energy is probably not high enough to interrupt the tetrahedral framework.

Summary

The crystal structure of fully hydrated heulandite-clinoptilolite from Succor Creek, Oregon, (25.5 H_2O pfu) was determined and refined in space group $C2/m$ at 100 K; a second harmonic generation powder test confirmed the sample to be centric and space group $C2/m$ to be correct. Next, four dehydration experiments performed under dry N_2, with associated structure refinements, were conducted to determine the mechanism of H_2O release in natural heulandite-clinoptilolite. At room temperature, flushing the crystal with dry N_2 resulted in expulsion of 8 H_2O pfu. The released H_2O was partially H bonded to the channel walls (space-filling H_2O) and partially originated from H_2O coordinating Na, the evolved H_2O lost first during dehydration. As H_2O coordinating Na was lost, the Na migrated closer to the cavity wall of the A channel.

An additional dehydration mechanism was observed in the B channel where the coordination with O of Ca was reduced from eight to seven. Just 1 h at 473 K in a dry-N_2 atmosphere was sufficient to produce a heat-collapsed structure with strongly compressed channel systems and 4–5 H_2O pfu (ca.). This heat-collapsed structure possesses the same tetrahedral topology as the natural sample. Ca adopted a different position in the B channel and is coordinated to 2 H_2O and 4 O atoms from the tetrahedral framework. The H_2O coordinating Na was lost and the Na nestled at the cavity wall.

The structural investigations support the statements of Bish (1988): (1) exchangeable cations have a profound influence on the dehydration behavior, (2) it is more ap-

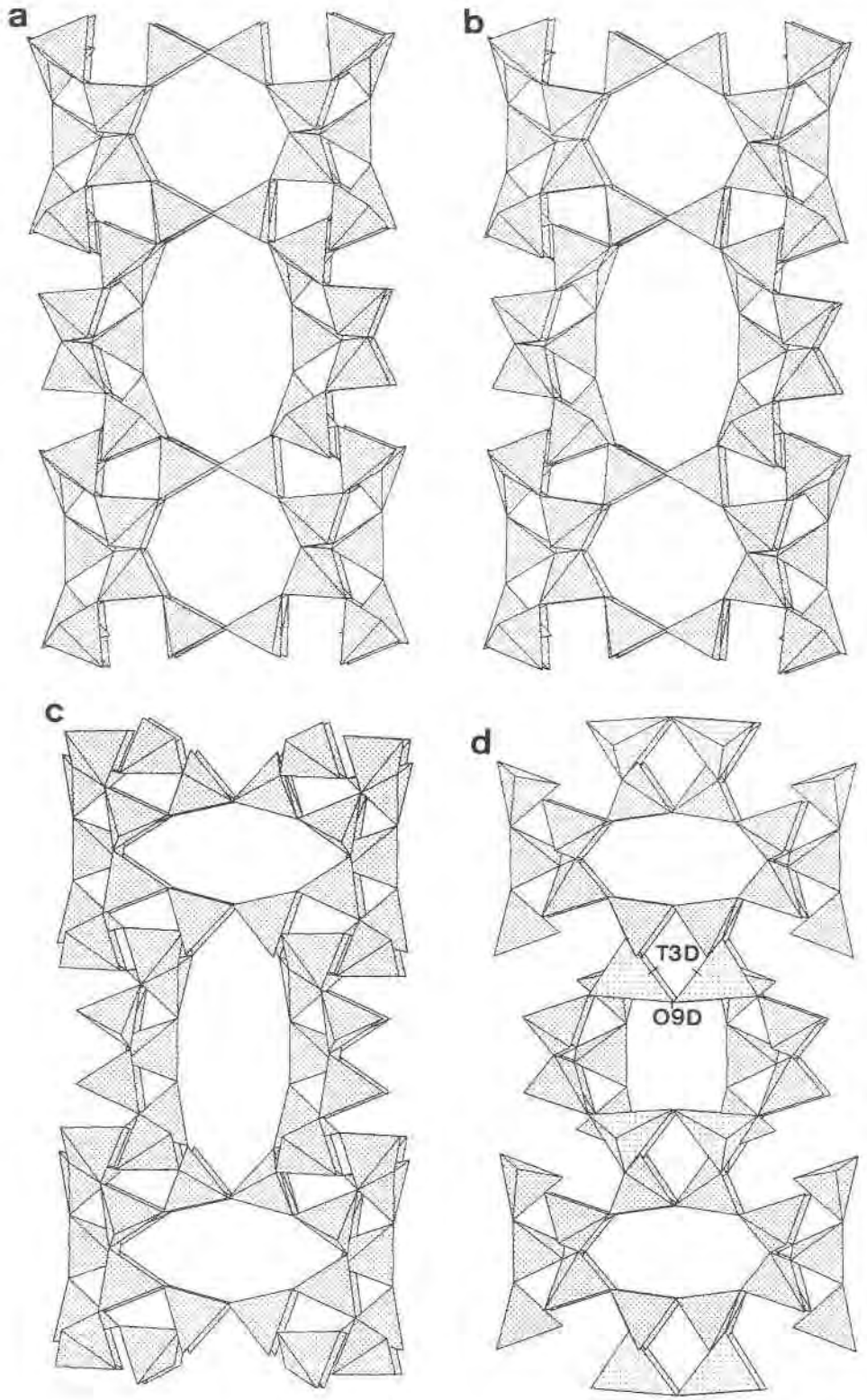

Fig. 3. Projection inclined 2° from [001] displaying the tetrahedral framework at various degrees of dehydration. (**a**) Natural sample; (**b**) dehyd2 sample; (**c**) dehyd4 (heat-collapsed) sample; (**d**) sample Nadap, phase B (Alberti and Vezzalini, 1983).

propriate to speak of a continuum of H_2O-molecule binding energies than to refer to loosely bound or tightly bound zeolitic H_2O, and (3) univalent cations dehydrate more easily than divalent cations.

The cell parameters decrease with dehydration, with b decreasing the most. If exposed to high humidity the heat-collapsed phase of the Succor heulandite-clinoptilolite rehydrates rapidly to a hydrated phase. This can be derived from the change of cell dimensions.

Acknowledgments

We would like to dedicate this paper to F.D. Bloss, past president of MSA and former editor of the *American Mineralogist,* for his many contributions to teaching and research in mineralogy.

The authors wish to thank Charles R. Knowles of the Idaho Geological Survey for microprobe analysis and Franklin F. Foit of Washington State University for assistance in the X-ray powder diffraction experiments. Also, we thank Laura E. Davis of Lawrence Livermore National Laboratory for the second harmonic generation test. The reviews and comments from A. Alberti, D.L. Bish, and J.R. Smyth improved the manuscript. M.E.G. wishes to thank the Laboratorium für chemische und mineralogische Kristallographie, Universität Bern, for financial support while in Switzerland and the opportunity to perform this study. In Idaho, financial support was provided to M.E.G. by the Idaho Research Council and the State of Idaho National Science Foundation–EPSRCoR grant R11-8902065.

References cited

Alberti, A. (1972) On the crystal structure of the zeolite heulandite. Tschermaks Mineralogische und Petrographische Mitteilungen, 18, 129–146.

——— (1973) The structure type of heulandite B (heat-collapsed phase). Tschermaks Mineralogische und Petrographische Mitteilungen, 19, 173–184.

——— (1975) The crystal structures of two clinoptilolites. Tschermaks Mineralogische und Petrographische Mitteilungen, 22, 25–37.

Alberti, A., and Vezzalini, G. (1983) The thermal behaviour of heulandites: A structural study of the dehydration of the Nadap heulandite. Tschermaks Mineralogische und Petrographische Mitteilungen, 31, 259–270.

Alietti, A. (1972) Polymorphism and crystal chemistry of heulandites and clinoptilolites. Tschermaks Mineralogische und Petrographische Mitteilungen, 21, 291–298.

Alietti, A., Brigatti, M.F., and Poppi, L. (1977) Natural Ca-rich clinoptilolites (heulandites of group 3): New data and review. Neues Jahrbuch für Mineralogie Monatshefte, 1977, 493–501.

Benashvili, E.M., Uchaneishvili, T.G., and Charkviani, T.N. (1988) Adsorptive removal of sulphur organic compounds of oil by natural and acid modified clinoptilolites. In D. Kallo and H.S. Sherry, Eds., Occurrence, properties, and utilization of natural zeolites, p. 589–597. Akademiai Kiado, Budapest.

Bish, D.L. (1984) Effects of exchangeable cation composition on the thermal expansion/contraction of clinoptilolite. Clays and Clay Minerals, 32, 444–452.

——— (1988) Effects of composition on the dehydration behavior of clinoptilolite and heulandite. In D. Kallo and H.S. Sherry, Eds., Occurrence, properties, and utilization of natural zeolites, p. 565–576. Akademiai Kiado, Budapest.

Boles, J.R. (1972) Composition, optical properties, cell dimensions, and thermal stability of some heulandite-group zeolites. American Mineralogist, 57, 1452–1493.

Bresciani-Pahor, N., Calligaris, M., Nardin, G., Randaccio, L., Russo, E., and Comin-Chiaromonti, P. (1980) Crystal structure of a natural and a partially Ag-exchanged heulandite. Journal of the Chemical Society, Dalton Transactions, 1980, 1511–1514.

Enraf-Nonius (1983) Structure determination package (SDP). Enraf-Nonius, Delft, The Netherlands.

Galabova, I.M., and Haralampiev, G.A. (1988) Polymineral rocks as sorbents for oxygen enrichment of air. In D. Kallo and H.S. Sherry, Eds., Occurrence, properties, and utilization of natural zeolites, p. 577–587. Akademiai Kiado, Budapest.

Galli, E., Gottardi, G., Mayer, H., Preisinger, A., and Passaglia, E. (1983) The structure of a potassium-exchanged heulandite at 293, 373 and 593 K. Acta Crystallographica, B39, 189–197.

Gottardi, G., and Galli, D. (1985) Natural zeolites, 409 p. Springer-Verlag, Berlin.

Hambley, T.W., and Taylor, J.C. (1984) Neutron diffraction studies on natural heulandite and partially dehydrated heulandite. Journal of Solid State Chemistry, 54, 1–9.

Koyama, K., and Takéuchi, Y. (1977) Clinoptilolite: The distribution of potassium atoms and its role in thermal stability. Zeitschrift für Kristallographie, 145, 216–239.

Mason, B., and Sand, L.B. (1960) Clinoptilolite from Patagonia: The relationship between clinoptilolite and heulandite. American Mineralogist, 45, 341–350.

Merkle, A.B., and Slaughter, M. (1968) Determination and refinement of the structure of heulandite. American Mineralogist, 53, 1120–1138.

Mortier, W.J., and Pearce, J.R. (1981) Thermal stability of the heulandite-type framework: Crystal structure of the calcium/ammonium form dehydrated at 483 K. American Mineralogist, 66, 309–314.

Mumpton, F.A. (1960) Clinoptilolite redefined. American Mineralogist, 45, 351–369.

——— (1978) Natural zeolites: A new industrial mineral commodity. In L.B. Sand and F.A. Mumpton, Eds., Natural zeolites: Occurrence, properties, use, p. 3–27. Pergamon, New York.

——— (1988) Development of uses for natural zeolites: A critical commentary. In D. Kallo and H.S. Sherry, Eds., Occurrence, properties, and utilization of natural zeolites, p. 333–365. Akademiai Kiado, Budapest.

Sheldrick, G.M. (1976) SHELX76. Program for crystal structure determination. University of Cambridge, England.

——— (1986) SHELX-86. Fortran-77 program for the solution of crystal structures from diffraction data. Institut für Anorganische Chemie der Universtät Göttingen, Germany.

Smyth, J.R., Spaid, A.T., and Bish, D.L. (1990) Crystal structures of a natural and a Cs-exchanged clinoptilolite. American Mineralogist, 75, 522–528.

Manuscript received December 10, 1990
Manuscript accepted June 26, 1991